Heterogeneity in the Conformation of Valine in the Elastin Mimetic $(LGGVG)_6$ as Shown by Solid-State ^{13}C NMR Spectroscopy

Kosuke Ohgo,[†] Walter P. Niemczura,[‡] Jun Ashida,[§] Michi Okonogi,[†] Tetsuo Asakura,*[,†] and Kristin K. Kumashiro*[,‡]

Department of Biotechnology, Tokyo University of Agriculture and Technology, Koganei, Tokyo 184-8588, Japan, Department of Chemistry, University of Hawaii, 2545 McCarthy Mall, Honolulu, Hawaii 96822, and Varian Technologies Japan Ltd., Minato-ku, Tokyo 108-0023, Japan

Received July 21, 2006; Revised Manuscript Received September 29, 2006

Elastin is an abundant protein found in vertebrates and is the source of elasticity in connective tissues and blood vessels. The repeating polypeptide sequences found in the hydrophobic domains of elastin have been the focus of many studies that attempt to understand the function of the native protein on a molecular scale. In this communication, the $(LGGVG)_6$ elastin mimetic is characterized by solid-state ^{13}C NMR spectroscopy. Through the use of a combination of a statistical analysis based on the Protein Data Bank, one-dimensional cross-polarization magic-angle-spinning NMR spectroscopy, and two-dimensional off-magic-angle-spinning spin-diffusion experiments, it is determined that this tandem repeat does not form a regular, highly ordered structure. Instead, like the poly(VPGVG) elastin mimetics, the valine has a twofold heterogeneity, although the conformations of these two populations differ from one peptide to the other.

Introduction

Elasticity in vertebrate tissue typically originates from the protein *elastin*, a cross-linked protein with an amino acid composition dominated by small hydrophobic residues, especially glycine. Elastin and its soluble monomer *tropoelastin* have been described as having two domain types, hydrophobic and cross-linking.[1] The former includes an abundance of repeating polypeptidyl sequences, of which significant interest has focused on the poly(Val-Pro-Gly-Val-Gly) or $(VPGVG)_n$ motif.[2,3] However, there are other tandem repeats that are present in these domains, including the poly(LGGVG) or other poly(GGXG) peptides.[4] Structure−function studies have typically focused on the tandem repeats of the hydrophobic domains of elastin, with the hypothesis that elasticity arises from these regions.[2,5] The cross-linking regions are alanine-rich, interspersed with lysines (in the monomer) and/or covalent cross-links (in the mature protein).

Although clearly essential for the proper function of the organism, there is a dearth of high-resolution structural information available for this protein. Earlier, extensive studies by Urry indicated that the repeating polypeptides folded into β-turns,[6,7] while others indicated that more complex models were necessary.[8−11] The complications for completing high-resolution structural studies with crystallography and solution NMR spectroscopy stem from the native protein's extensive hydrophobicity and the presence of cross-links, respectively. Hence, the use of solid-state NMR spectroscopy as a tool for the elucidation of structural and dynamic information on elastin provides a novel and powerful glimpse into the molecular organization of the protein.

In our laboratories[8,12−18] as well as others,[9,19] solid-state NMR has been used to show that there is likely a significant degree of heterogeneity in elastin as well as in mimetics of its hydrophobic domains. Solid-state NMR approaches have ranged from the very straightforward, such as one-dimensional (1D) cross-polarization with magic-angle-spinning (CPMAS) ^{13}C NMR spectroscopy and related relaxation measurements,[13,16] to significantly more sophisticated methods such as rotational echo double resonance and two-dimensional (2D) methods for the determination of internuclear distances and torsion angles, respectively.[8,12] These results have shown that structures such as the β-spiral[6,7] are likely not the prevalent conformation in the solid state for this tandem repeat. Of all the repeating sequences in elastin, (VPGVG) polypeptides have been most extensively characterized by solid-state NMR spectroscopy. Again, however, it has been noted[4] that there are other repeating peptide sequences in the hydrophobic domains of elastin, of which the glycine-rich $(LGGVG)_n$ polypeptide is one.

The $(LGGVG)_n$ polypeptide has been previously shown to be a good mimetic for soluble elastin peptides and, as an aggregate, for mature elastin.[5] Specifically, Tamburro and coworkers have demonstrated that this repeating polypeptide forms aggregates that closely mimic that of the native elastin. In addition, Debelle and Tamburro have suggested that the (XGGXG)-type repeats bear stronger relevance in the determination of structure−function models for elastin than the (VPGVG) repeats, as they more clearly illustrate the "sliding β-turn" model. However, very little detailed structural information is available for this polypeptide, particularly in the solid state. In an earlier solid-state NMR study, it was shown that the $(LGGVG)_n$ polypeptide ($n = 2-15$) is structurally heterogeneous; i.e., there are at least two different conformers present in this elastin mimetic.[14] The 1D ^{13}C CPMAS NMR spectrum clearly showed two peaks for the Val-Cβ site, with the major population at 32.7 ppm and a minor one at 29.2 ppm. Additionally, deconvolution of the backbone carbonyl line shape

* Authors to whom correspondence should be addressed. Phone/Fax: +81-42-383-7733 (T.A.). Phone: (808) 956-5733 (K.K.K.). Fax: (808) 956-5908 (K.K.K.) E-mail: asakura@cc.tuat.ac.jp; kumashir@hawaii.edu.

[†] Tokyo University of Agriculture and Technology.

[‡] University of Hawaii.

[§] Varian Technologies Japan Ltd.

10.1021/bm0607168 CCC: $33.50
Published on Web 11/14/2006

provided little support for any type of structural model that was highly ordered. As these experiments were done on natural-abundance ^{13}C populations, however, little high-resolution information could be obtained.

In this communication, the valines of the hydrophobic regions of elastin are targeted for studies that yield high-resolution structural information. Here, samples of $(LGGVG)_6$ are characterized by solid-state ^{13}C NMR spectroscopy. The isotropic chemical shifts, again obtained from 1D CPMAS, are used to place constraints[20−23] on the Ramachandran plot for allowed valine conformations. The 1D data is complemented by a statistical analysis based on structures from the Brookhaven Protein Data Bank (PDB). Two-dimensional spin diffusion under off-magic-angle-spinning (OMAS) conditions is also obtained for an isotopically enriched sample. A "conformational ensemble",[5] or a mixture of conformations, best describes the pattern obtained in the 2D OMAS spin-diffusion experiment. These results are consistent with work from this group and others and provide additional support for an emerging model in elastin structure−function.

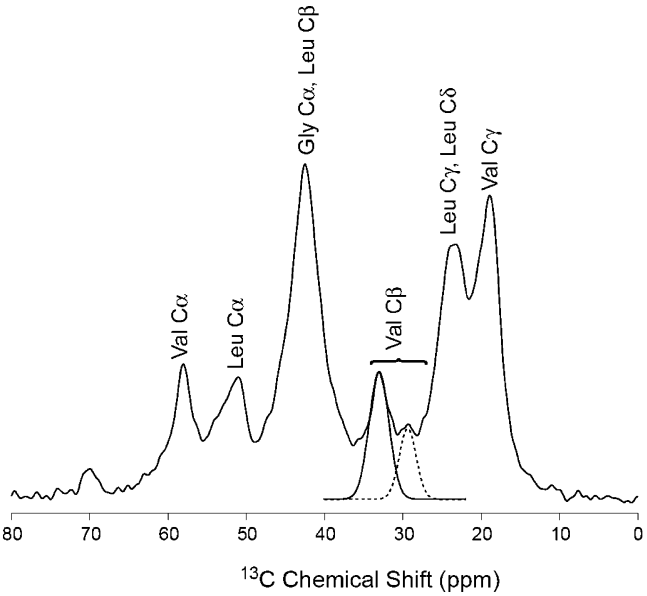

Figure 1. One-dimensional ^{13}C CPMAS NMR spectrum (aliphatic region) of $(LGGVG)_2LG[1\text{-}^{13}C]G^{13}[1\text{-}^{13}C]V^{14}G(LGGVG)_3$ with peak assignment. A total of 600 scans were accumulated, and the spectrum was processed with 40 Hz Lorentzian line broadening. The deconvolution of the Val-Cβ peak was shown: major component (solid line) and minor component (broken line). The rationale for the assignment of peaks is given in ref 14.

Experimental Section

Peptide Synthesis. The elastin model polypeptide $(LGGVG)_6$ and the doubly labeled $(LGGVG)_2LG[1\text{-}^{13}C]G[1\text{-}^{13}C]VG(LGGVG)_3$ were prepared by solid-phase Fmoc chemistry[24] on a fully automated Pioneer Peptide Synthesis System (Applied Biosystems Ltd., Warrington, U. K.). Unlabeled Fmoc amino acids, the resin, *O*-(7-azabenzotriazole-1-yl)-*N*,*N*,*N*′*N*′-tetramethyluronium hexafluorophosphate (HATU), and *N*,*N*-diisopropylethylamine (DIEA) were purchased from Applied Biosystems. The solvents of high-purity grade and other chemicals were available from Wako Pure Chemical Industries Ltd., Osaka, Japan. The ^{13}C-labeled amino acids [1-^{13}C]Gly (99%) and L-[1-^{13}C]Val (99%) (Cambridge Isotope Laboratories, Inc., Andover, MA) were also used. Typically the peptide was assembled on Fmoc-Gly-PEG-PS resin. The coupling of Fmoc amino acids was performed using HATU. After synthesis, the free peptides were released from the resin by treatment with a mixture of trifluoroacetic acid, phenol, triisopropylsilane, and water (88:5:2:5 vol %) for 2 h at room temperature. The crude peptide was precipitated with dry diethyl ether and washed repeatedly with cold ether. The precipitate, collected by centrifugation, was dried in vacuo and purified by high-performance liquid chromatography using acetonitrile as the eluent. After purification, acetonitrile was removed by evaporation at 42 °C followed by lyophilization for 24 h.

Solid-State NMR Spectroscopy. The solid-state NMR experiments were performed on Varian Unity Inova spectrometers at Varian Technologies, Japan, and at the University of Hawaii. Both spectrometers have a ^1H resonance frequency of 400 MHz and are each equipped with a 7 mm double-resonance Jakobsen-type MAS probe. For these experiments, 53 mg of the enriched $(LGGVG)_6$ peptide was packed into a 7 mm rotor. The sample was restricted with plugs to the middle 5 mm of the rotor, to minimize radio frequency inhomogeneity effects. The sample spinning rate was 6 kHz (±3 Hz) for both 1D and 2D experiments. Chemical shifts are externally referenced to adamantane ($\delta(^{13}C) = 28.8$ ppm).

For the 1D experiments, parameters for cross-polarization (CP)[25] are a 7.0 μs ^1H 90° pulse followed by a 1.5 ms contact time ($\gamma B_1/2\pi = 45$ kHz during CP, using a constant amplitude) with a 5 s recycle delay. Two-pulse phase modulation (TPPM) decoupling ($\gamma B_1/2\pi = 75$ kHz) was applied during acquisition.

For CP in the 2D experiments, a 7.0 μs ^1H 90° pulse was followed by a 1.5 ms contact time ($\gamma B_1/2\pi = 36$ kHz during CP). The CP is constant-amplitude, as with the 1D experiments. TPPM decoupling ($\gamma B_1/2\pi = 58$ kHz) was used during acquisition in t_2. A mixing time of 2 s was used after optimization. This duration allows for spin diffusion between intramolecular (not intermolecular) carbon atoms of selectively isotopically labeled Val and Gly residues. For the 2D spin-diffusion experiments, the "off-magic-angle" condition was $\theta = \theta_m - 5.9°$; where θ_m is magic angle. The scaling factor used was $^1/_2(3\cos^2(\theta - 1) = +0.15$. The angle θ (between the static magnetic field and the sample spinning axes) and the scaling factor were determined by measuring the (scaled) ^{13}C chemical shift anisotropy (CSA) of hydroquinone under OMAS conditions. The CSA of the unsubstituted aromatic carbon of hydroquinone is 176 ppm. A total of 600 scans were taken for each of the 64 pairs of time increments, implementing phase-sensitive 2D acquisition via the States method. The acquisition times were 12 and 0.7 ms in the direct and indirect dimensions, respectively. A 3 s relaxation delay between scans was used for a total experiment time of 117 h. The data were processed using 50 Hz Gaussian line broadening in both time domains and zero-filling the data to a final size of 1024 × 1024 data points. More details on the theory and the pulse sequence are found in the literature.[26−29]

PDB Analysis. The torsion angles in the Gly-Val-Gly (GVG) sequence in proteins and peptides were obtained from the X-ray crystallographic data in the Protein Data Bank at the Research Collaboratory for Structural Bioinformatics (http://www.rcsb.org/pdb/). For this analysis, only the structures at 2.0 Å resolution or better and with a *R* factor ≤20% were used. A subset of 329 GVG occurences were obtained from the database after excluding multiple entries of proteins with a similarity greater than 50%. For each unique GVG-containing peptide or protein, the torsion angles involving the Val-Cα and Val-Cβ carbons were calculated from the atomic coordinate files and then plotted on the respective Ramachandran maps.

Analysis of the ^{13}C Chemical Shift Map. The empirical relationship between ^{13}C chemical shifts and torsion angles in proteins[22,23] was used to impose additional constraints on the allowed conformations of this peptide.[26,30] The $^{13}C\alpha$ and $^{13}C\beta$ chemical shifts for valines in the peptide were obtained from the 1D CPMAS data, as shown in Figure 1. Then, for each coordinate (ϕ,ψ) in the Ramachandran map, the respective $C\alpha_{map}$ and $C\beta_{map}$ were determined, using the methodology presented in ref 23. The root-mean-square (rms) errors, Δ, are used to provide a quantitative basis for identifying the most likely torsion angles for a residue with observed ^{13}C chemical shifts for the Cα and Cβ carbons. The Δ values are calculated as

$$\Delta = \left\{ \frac{(C\alpha - C\alpha_{map})^2 + (C\beta - C\beta_{map})^2}{2} \right\}^{1/2}$$

Simulation of 2D Spin-Diffusion NMR Spectra. Simulated spectra were produced using a program developed in the Asakura laboratory. Details are described elsewhere.[26] Briefly, calculations were done on an OCTANE (Silicon Graphics, Inc.) workstation, using an incremental grid of 15° for each of the angles, ϕ and ψ. Diagonal peaks were neglected in the best-fit analysis. The root-mean-square deviation (rmsd) for each (ϕ,ψ) pair is defined as

$$\mathrm{rmsd}(\phi,\psi) = \sqrt{\frac{\sum_{i=1}^{N} [E_i - \lambda(\phi,\psi) S_i(\phi,\psi)]^2}{N}}$$

where N is the number of intensities analyzed, E_i are the experimental intensities, $S_i(\phi,\psi)$ are the calculated intensities, and $\lambda(\phi,\psi)$ is a optimal scaling factor calculated to minimize the rmsd at each (ϕ,ψ) pair.[31] Visualization of the spectra and rmsd calculations were done using MATLAB (The MathWorks, Inc.).

Results and Discussion

Verification of Similarity of Structures in Poly(LGGVG) and (LGGVG)$_6$ from 1D CPMAS NMR Experiments. Solid-state 1D ^{13}C CPMAS NMR spectra indicate that (LGGVG)$_6$ is essentially identical to the larger and more heterogeneous polypeptide (LGGVG)$_n$, based on the chemical shifts and the relative intensities of the respective features. Previously, Kumashiro and co-workers showed that the 1D ^{13}C CPMAS NMR spectrum of the natural-abundance ^{13}C population of the elastin-like polypeptide (LGGVG)$_n$ (n = 2−15) has a two-component nature at the C$_\beta$-Val site; i.e., the relative ratio of the downfield peak (32.7 ppm) to the upfield peak (29.2 ppm) was found to be roughly 2:1.[14] Figure 1 shows the 1D ^{13}C CPMAS NMR spectrum of the aliphatic region of enriched (LGGVG)$_6$. The deconvolution of the Val-Cβ carbon feature is also illustrated. The Val-Cα carbon has a chemical shift of 58 ppm. There are two peaks for the Val-Cβ carbon, one with a chemical shift of 32.7 ppm (70%) and the other with a chemical shift of 29.2 ppm (30%). Hereafter, the populations corresponding to these shifts are called the "major" and "minor" conformations, respectively. Note that peak intensities are quantitative, with certain caveats, namely, that the relative populations are determined for two conformers of the Val-Cβ of (LGGVG)$_6$; i.e., such conclusions would not be reasonable if we were comparing intensities of a methine carbon (such as Val-Cα) with that of a methyl, as the mechanisms for CP transfer and relaxation differ. However, for two populations of the same site in the same residue, such differences are negligible. As a final consideration, we note that the spectra and relative intensities of the peaks of interest do not change significantly at elevated (45 °C) and lower (−20 °C) temperatures (not shown). A 2D MAS exchange experiment also confirms that conformational exchange does not take place in the regime of 500 ms or less (also not shown). The variable-temperature and MAS exchange experiments all support the picture of two distinct, nonexchanging populations of valine in (LGGVG)$_6$.

Ramachandran Plots Restricted by Isotropic Chemical Shifts. Generally speaking, highly populated regions in the Ramachandran map, based on the results of the PDB search, are identified as more or less likely in the target system, in our case (LGGVG)$_6$, by imposing additional constraints provided by the isotropic chemical shift information. The valines found in GVG-containing PDB structures occur with the torsion angles shown in the contour plot of Figure 2. The most highly populated angles (ϕ,ψ) in the Ramachandran plot are centered at (−60°,−45°), (−75°,−15°), (−110°,135°), and (−140°,150°). These regions are relatively broad, and secondary maxima are also present, such as the one at (−120°,20°).

A quantitative approach is shown in Figure 2, illustrating the combined chemical Cα and Cβ chemical shifts error map for the Val residues superimposed upon the PDB result. Previously, Asakura and Williamson have demonstrated that the strong correlation between isotropic chemical shift and secondary structure can be extended to the determination of high-resolution structural parameters, such as torsion angles ϕ and ψ.[22] Hence, the rms error for each pair of torsion angles (ϕ,ψ) can be calculated for a site with a given chemical shift. The solid lines in Figure 2 illustrate the regions of lowest rms error (i.e., Δ = 0.5 and 1). The regions of greatest overlap between the calculated rms errors and the PDB-derived contour plots are indicated for the major (δ(Val-^{13}Cβ) = 32.7 ppm, Figure 2a) and minor (δ(Val-^{13}Cβ) = 29.2 ppm, Figure 2b) populations of the Val residues with the red and blue boxes, respectively. This analysis shows that the major valine population has torsion angles of (−150° ≤ ϕ ≤ −90°, 105° ≤ ψ ≤ 165°), whereas the minor valine population has torsion angles of (−150° ≤ ϕ ≤ −90°, 0° ≤ ψ ≤ 60°).

On the basis of our approach, likely secondary structures are identified for the two populations of valine in the central subunit of (LGGVG)$_6$. The major population, with a ^{13}C chemical shift of 32.7 ppm, corresponds to β-sheet or polyproline II structures. The minor population, with a ^{13}C shift of 29.2 ppm, is assigned to a type-I β-turn structure. The peak at 58 ppm, corresponding to Val-^{13}Cα, suggests either a β-sheet or polyproline II (PPII) structure, which is reasonably consistent with the assignments made for the Cα carbon of the polypeptide. As a reference point, the random coil chemical shifts for Val-Cα and Val-Cβ are 60.5 and 31.2 ppm, respectively.[32]

Mixture of Two Conformations Consistent with 2D OMAS Spin-Diffusion NMR Results. Direct observation of the torsion angles in the peptide are possible with isotopically enriched samples. To obtain this information, a 2D spin-diffusion experiment under OMAS conditions is employed.[26,33] Figure 3a shows the spectrum obtained for the doubly labeled polypeptide (LGGVG)$_2$LG[1-^{13}C]G^{13}[1-^{13}C]V^{14}G(LGGVG)$_3$. In this sample, the backbone carbonyls of Gly-13 and Val-14 are ^{13}C-labeled. The best-fit simulated spectrum, shown in Figure 3b, is obtained using a combination of torsion angles, as expected from the 1D results. A single set of (ϕ,ψ) angles does not yield a spectrum that resembles the experimentally obtained one. Instead, the best-fit simulation is found using a mixture of two conformations.

Through the use of the constraints derived from the relative intensities and chemical shifts in the 1D ^{13}C CPMAS spectrum and the PDB analysis, the 2D spin-diffusion spectra were calculated for a mixture of two conformations for a limited range of ϕ and ψ angles. It is known that two distinct but unequally populated conformers are needed for the simulation. To obtain the best-fit simulation, simulation procedures were utilized with the results obtained from the chemical shift analysis and the deconvolution, as detailed above. The chemical shift analysis was used to obtain limits for the torsion angles for the major (−150° ≤ ϕ ≤ −90°, 105° ≤ ψ ≤ 165°) and minor (−150° ≤ ϕ ≤ −90°, 0° ≤ ψ ≤ 60°) populations. A grid of possible structures was generated for the major population, using 15°

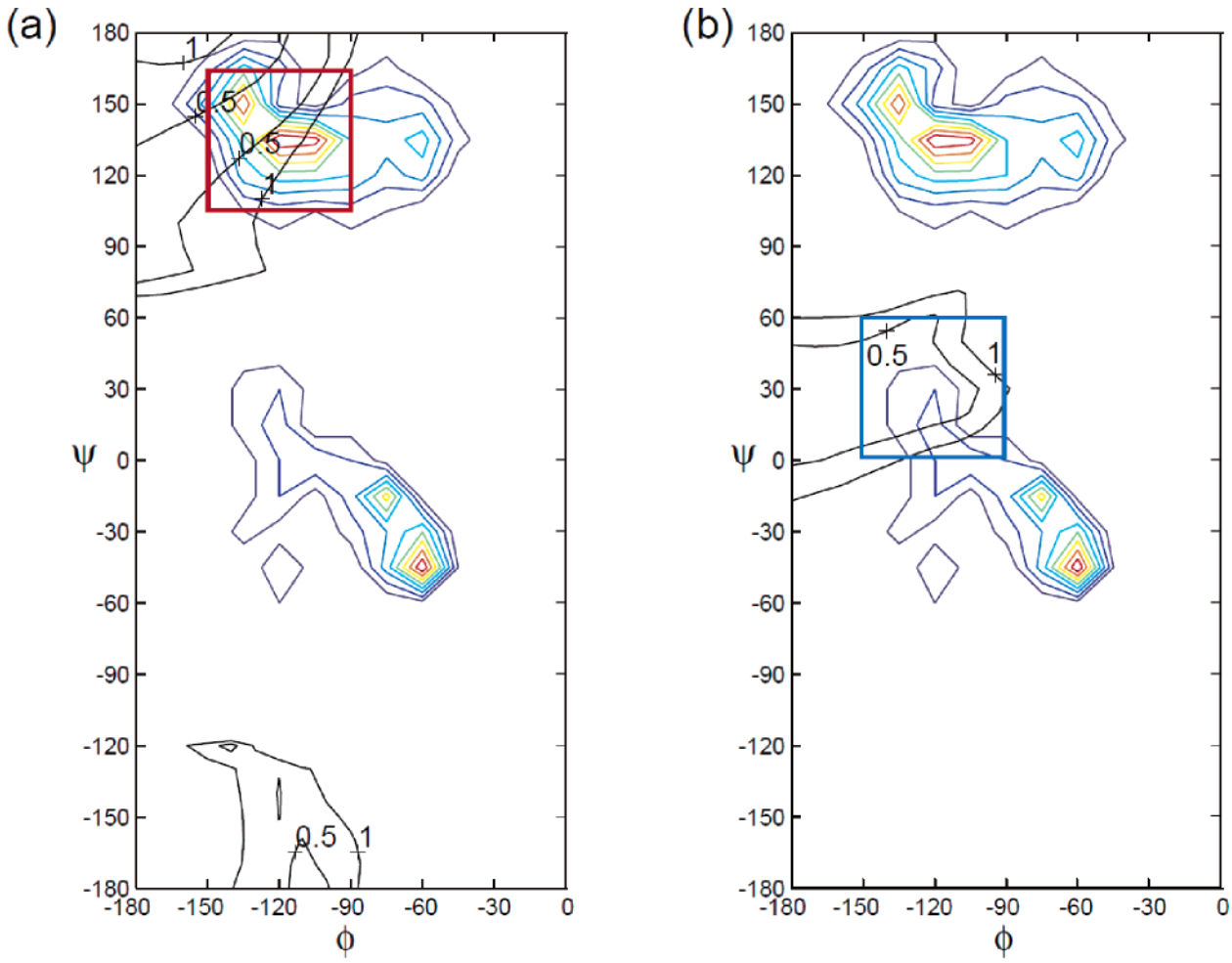

Figure 2. Contour plot of the PDB results for Val in (GVG) with results of the combined chemical shift error analysis. The values of the rmsd error $\Delta = 0.5$ and $\Delta = 1.0$ are denoted with the gray scale contours. The regions of greatest overlap are indicated with red and blue boxes for the (a) major and (b) minor populations, respectively.

increments, to obtain 25 (5×5) exchange patterns that corresponded to the range of torsion angles from the chemical shift analysis. A similar approach was done for the minor population. Then, another grid of exchange patterns was obtained; in this case, 625 (25×25) patterns were calculated, using a weight of 0.7 for the major and 0.3 for the minor. The weight of each conformer had been estimated from the deconvolution of the 1D ^{13}C CPMAS spectrum. The best fit is obtained with major population torsion angles of $(\phi,\psi) = (-105°,135°)$ and minor conformation torsion angles of with $(\phi,\psi) = (-120°, 30°)$. These values are consistent with the information obtained with the coupled PDB−chemical shift analysis.

Conclusion

The local structure of the valine in a central subunit of the polypeptide $(LGGVG)_6$ was determined using a combination of empirical and experimental methods. The torsion angles of the central Val residue of the (GVG) motif was first compiled from the PDB, and then the field of possible conformations was narrowed using the isotropic chemical shifts from the 1D CPMAS experiments. Then, the 2D OMAS spin-diffusion NMR experiment was conducted on a doubly ^{13}C-labeled sample of the $(LGGVG)_6$ polypeptide, and the best-fit simulation was obtained. The results obtained for both the backbone and the side chain regions of the central valine residue provide strong evidence for the presence of at least two types of conformations, even in this simplified polypeptide.

Early models for the hydrophobic repeats of elastin called for highly regularized structures, such as the β-spiral, a series of repeating type-II β-turns.[6,7] More recently though, this group and others have shown that the most likely scenario for the more commonly observed $(VPGVG)_n$ elastin mimetic is that of a "bimodal distribution"[9] or "conformational ensemble".[8] We find a similar scenario is most likely present in this related mimetic $(LGGVG)_6$ and the related $(LGGVG)_n$. Specifically, the analogous Val-14 residue of the doubly ^{13}C-labeled $(VPGVG)_6$ had a bimodal structure distribution, or two populations, with the major one (70%) having approximate torsion angles of $(\phi, \psi) = (-110°,130°)$ and the minor conformation (30%) with torsion angles of $(\phi, \psi) = (-75°,15°)$.[8] Interestingly, the conformation of the major population of $(VPGVG)_6$ is similar to that of $(LGGVG)_6$, whereas that of the minor differs between the two types of hydrophobic repeats.

The finding of the conformational ensemble in $(LGGVG)_6$ also coincides with recent work of Tamburro and co-workers,[34] who described the structural features of the individual exons of human tropoelastin using circular dichroism and solution ^1H NMR spectroscopy. The LGGVG-type sequence is found in the hydrophobic domain encoded by exon 28. Exon 28 exhibits features of a PPII-type structure in water and type-I β-turn in trifluoroethanol, and Tamburro and co-workers concluded that the dependence of structure on "microenvironment" provides

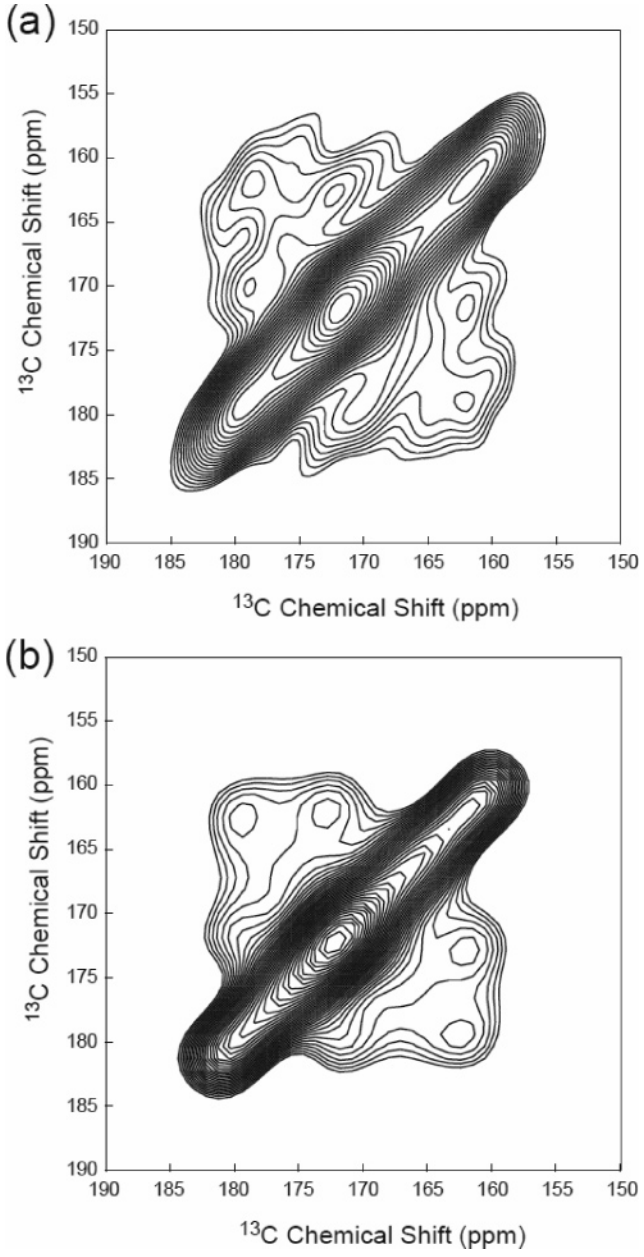

Figure 3. (a) Experimental and (b) best-fit simulated 2D OMAS spin-diffusion spectra of $(LGGVG)_2LG[1\text{-}^{13}C]G^{13}[1\text{-}^{13}C]V^{14}G(LGGVG)_3$, the $(LGGVG)_6$ polypeptide with ^{13}C labels at the carbonyl carbons of Gly-13 and Val-14.

excellent support for models of elastin that rely on conformational equilibria. As such, these results on the simplified elastin mimetic are consistent with the findings of the sequence in the individual domain, bringing new support to the usage of simple tandem repeats in the study of this novel protein's structure–function relationships.

Acknowledgment. This work was partially supported by grants to K.K.K. from the National Science Foundation (Grant No. MCB-0344975) and the National Institutes of Health (Grant No. RR 16453). T.A. acknowledges supports from the Insect Technology Project, Japan, and Agriculture Biotechnology Project, Japan.

References and Notes

(1) Rosenbloom, J.; Abrams, W. R.; Mecham, R. *FASEB J.* **1993**, *7*, 1208–1218.
(2) Urry, D. W. *J. Protein Chem.* **1988**, *7*, 1–34.
(3) Urry, D. W. *J. Phys. Chem. B* **1997**, *101*, 11007–11028.
(4) Debelle, L.; Tamburro, A. M. *Int. J. Biochem. Cell Biol.* **1999**, *31*, 261–272.
(5) Martino, M.; Coviello, A.; Tamburro, A. M. *Int. J. Biol. Macromol.* **2000**, *27*, 59–64.
(6) Urry, D. W.; Trapane, T. L.; Sugano, H.; Prasad, K. U. *J. Am. Chem. Soc.* **1981**, *103*, 2080–2089.
(7) Venkatachalam, C. M.; Urry, D. W. *Macromolecules* **1981**, *14*, 1225–1229.
(8) Ohgo, K.; Ashida, J.; Kumashiro, K. K.; Asakura, T. *Macromolecules* **2005**, *38*, 6038–6047.
(9) Yao, X. L.; Hong, M. *J. Am. Chem. Soc.* **2004**, *126*, 4199–4210.
(10) Rodriguez-Cabello, J. C.; Alonso, M.; Diez, M. I.; Caballero, M. I.; Herguedas, M. M. *Macromol. Chem. Phys.* **1999**, *200*, 1831–1838.
(11) Li, B.; Alonso, D. O. V.; Daggett, V. *J. Mol. Biol.* **2001**, *305*, 581–592.
(12) Asakura, T.; Ashida, J.; Ohgo, K. *Polym. J.* **2003**, *35*, 293–296.
(13) Kumashiro, K. K.; Ho, J. P.; Niemczura, W. P.; Keeley, F. W. *J. Biol. Chem.* **2006**, *281*, 23757–23765.
(14) Kumashiro, K. K.; Kurano, T. L.; Niemczura, W. P.; Martino, M.; Tamburro, A. M. *Biopolymers* **2003**, *70*, 221–226.
(15) Perry, A.; Stypa, M. P.; Foster, J. A.; Kumashiro, K. K. *J. Am. Chem. Soc.* **2002**, *124*, 6832–6833.
(16) Perry, A.; Stypa, M. P.; Tenn, B. K.; Kumashiro, K. K. *Biophys. J.* **2002**, *82*, 1086–1095.
(17) Kumashiro, K. K.; Kim, M. S.; Kaczmarek, S. E.; Sandberg, L. B.; Boyd, C. D. *Biopolymers* **2001**, *59*, 266–275.
(18) Kumashiro, K. K.; Niemczura, W. P.; Kim, M. S.; Sandberg, L. B. *J. Biomol. NMR* **2000**, *18*, 139–144.
(19) Hong, M.; Isailovic, D.; McMillan, R. A.; Conticello, V. P. *Biopolymers* **2003**, *70*, 158–168.
(20) Birn, J.; Poon, A.; Mao, Y.; Ramamoorthy, A. *J. Am. Chem. Soc.* **2004**, *126*, 8529–8534.
(21) Wei, Y.; Lee, D. K.; Ramamoorthy, A. *J. Am. Chem. Soc.* **2001**, *123*, 6118–6126.
(22) Iwadate, M.; Asakura, T.; Williamson, M. P. *J. Biomol. NMR* **1999**, *13*, 199–211.
(23) Asakura, T.; Iwadate, M.; Demura, M.; Williamson, M. P. *Int. J. Biol. Macromol.* **1999**, *24*, 167–171.
(24) Carpino, L. A.; Han, G. Y. *J. Am. Chem. Soc.* **1970**, *92*, 5748–5749.
(25) Pines, A.; Gibby, M. G.; Waugh, J. S. *J. Chem. Phys.* **1973**, *59*, 569–590.
(26) Asakura, T.; Ashida, J.; Yamane, T.; Kameda, T.; Nakazawa, Y.; Ohgo, K.; Komatsu, K. *J. Mol. Biol.* **2001**, *306*, 291–305.
(27) Henrichs, P. M.; Linder, M. *J. Magn. Reson.* **1984**, *58*, 458–461.
(28) Edzes, H. T.; Bernards, J. P. C. *J. Am. Chem. Soc.* **1984**, *106*, 1515–1517.
(29) Bennett, A. E.; Ok, J. H.; Griffin, R. G.; Vega, S. *J. Chem. Phys.* **1992**, *96*, 8624–8627.
(30) Ashida, J.; Ohgo, K.; Komatsu, K.; Kubota, A.; Asakura, T. *J. Biomol. NMR* **2003**, *25*, 91–103.
(31) Weliky, D. P.; Bennett, A. E.; Zvi, A.; Anglister, J.; Steinbach, P. J.; Tycko, R. *Nat. Struct. Biol.* **1999**, *6*, 141–145.
(32) Wishart, D. S.; Bigam, C. G.; Holm, A.; Hodges, R. S.; Sykes, B. D. *J. Biomol. NMR* **1995**, *5*, 67–81.
(33) Ohgo, K.; Kawase, T.; Ashida, J.; Asakura, T. *Biomacromolecules* **2006**, *7*, 1210–1214.
(34) Tamburro, A. M.; Bochicchio, B.; Pepe, A. *Biochemistry* **2003**, *42*, 13347–13362.

BM0607168